AD-A244 291

ION PAGE

Form Approved
OMB No. 0704-0188

(2)

1. AGENCY USE ONLY (Leave blank)	2. REPORT DATE	3. REPORT TYPE AND DATES COVERED
	JUNE 20, 1991	TECHNICAL REPORT YR.I 2/1/90-1/31/91 Annual

4. TITLE AND SUBTITLE
KINETIC ASPECTS OF LATTICE MISMATCH IN MOLECULAR BEAM EPITAXICAL GROWTH ON PLANAR AND PATTERNED SUBSTRATES

5. FUNDING NUMBERS
AFOSR-90-0184

6. AUTHOR(S)
A. MADHUKAR

7. PERFORMING ORGANIZATION NAME(S) AND ADDRESS(ES)
UNIVERSITY OF SOUTHERN CALIFORNIA
DEPARTMENT OF MATERIALS SCIENCE AND ENGINEERING
SCHOOL OF ENGINEERING
LOS ANGELES, CA 90089-0241

8. PERFORMING ORGANIZATION REPORT NUMBER

9. SPONSORING/MONITORING AGENCY NAME(S) AND ADDRESS(ES)
AIR FORCE OFFICE OF SCIENTIFIC RESEARCH
ELECTRONIC AND MATERIALS SCIENCES DIRECTORATE
BOLLING AIR FORCE BASE
WASHINGTON, DC 20322

10. SPONSORING/MONITORING AGENCY REPORT NUMBER
23061-P1

11. SUPPLEMENTARY NOTES

DTIC
ELECTE
JAN 17 1992
D

92-01096

12a. DISTRIBUTION/AVAILABILITY STATEMENT

unlimited

This document has been approved for public release and sale; its distribution is unlimited.

13. ABSTRACT *(Maximum 200 words)*

This annual technical report summarizes the salient accomplishments during the first year. The work is focussed on examining the nature of the molecular beam epitaxical growth process, its control and optimization, achieving defect reduction via growth on prepatterned substrates, and the behaviour of some optical and transport characteristics for strained systems using InGaAs/AlGaAs as the vehicle. Highlights include (i) the first demonstration of GaAs(111)B homoepitaxy free of twins and with mirror-like surfaces through usage of real-time reflection electron diffraction intensity behaviour, (ii) demonstration of the presence of strain in the substrate to unexpectedly large depths below 3D islands of InGaAs, (iii) presence of atomic relaxation in coherent islands, (iv) the tendency for defect introduction at island edges beyond a critical size, (v) realization of strained InGaAs/AlAs resonant tunnelling diodes with room temperature peak currents ~ 125 kAmp/cm^2 and peak-to-valley ratios of 5:1, (vi) defect reduction via strain relief at mesa edges in growth on prepatterned mesas, (vii) realization of good electroabsorption in thick (1 μm to 2 μm) strained multiple quantum wells, (viii) dielectric encapsulation induced strain shifts, and (ix) rapid thermal annealing induced intermixing of components at interfaces and the resulting change in the nature of the quantum well potential.

14. SUBJECT TERMS	15. NUMBER OF PAGES
QUANTUM WELL STRUCTURES, MOLECULAR BEAM EPITAXY, REFLECTION ELECTRON DIFFRACTION, OPTIMIZED GROWTH KINETICS, μ-RAMAN RTDs PATTERNED SUBSTRATE GROWTH, ELECTROABSORPTION, DIELECTRIC ENCAPSULATION STRAINED EPITAXY, DEFECT REDUCTION.	32
	16. PRICE CODE

17. SECURITY CLASSIFICATION OF REPORT	18. SECURITY CLASSIFICATION OF THIS PAGE	19. SECURITY CLASSIFICATION OF ABSTRACT	20. LIMITATION OF ABSTRACT
unclass.	unclass.	unclass.	UL

92 1 13 010

ANNUAL SCIENTIFIC REPORT
AFOSR GRANT NO. AFOSR-90-0184

PERIOD: FEB. 01, 1990 - JAN. 31, 1991

KINETIC ASPECTS OF LATTICE MISMATCH IN MOLECULAR BEAM EPITAXICAL GROWTH ON PLANAR AND PATTERNED SUBSTRATES

SUBMITTED TO

AIR FORCE OFFICE OF SCIENTIFIC RESEARCH
ELECTRONIC AND MATERIALS SCIENCES DIRECTORATE
BOLLING AIR FORCE BASE
WASHINGTON, DC 20322

ATTN: MAJ. GERNOT POMERANKE

SUBMITTED BY

ANUPAM MADHUKAR
DEPARTMENT OF MATERIALS SCIENCE AND ENGINEERING
UNIVERSITY OF SOUTHERN CALIFORNIA
LOS ANGELES, CA 90089-0241

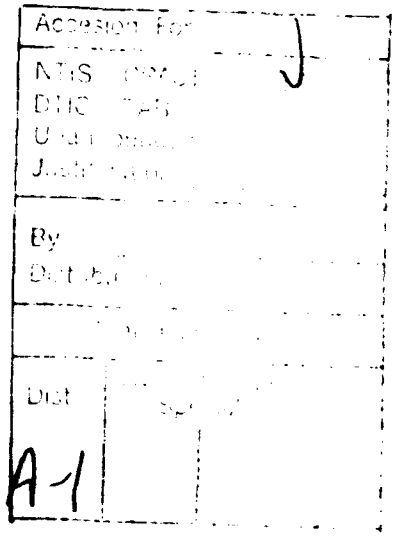

CONTENTS

ABSTRACT

This Annual Scientific Report provides a brief description of the accomplishments during the first year (Feb.1,1990-Jan.31,1991) of the AFOSR Grant No. AFOSR-90-0184.

I. SALIENT ACCOMPLISHMENTS

We provide in the following a summary of some of the significant results obtained during the first year of the above noted AFOSR grant. The details are to be found in the publications listed in Sec.III and referred to at appropriate places in the description given below.

I.1 GaAs(111)B HOMOEPITAXY:

An outstanding unsolved difficulty with the growth of GaAs on GaAs(111)B substrates had been the occurrence of pyramid-like surface structures and/or twins. We undertook to examine this phenomenon with a view to finding appropriate growth conditions under which twin-free and mirror-like surface may be simultaneously and reproducibly realized. This is the first critical step towards the growth of GaAs(111)B based heterostructures involving $Al_xGa_{1-x}As$ (i.e. unstrained) or $In_xGa_{1-x}As$ (i.e. strained) layers in which, it is believed, the existence of the piezoelectric effect may be fruitfully exploited for light modulators based on the quantum confined Stark effect (QCSE), apart from the predicted existence of non-linear optical effects.

Following our approach of systematic reflection high-energy electron diffraction (RHEED) studies to examine the correlation between growth conditions, growth kinetics, and the resulting nature of the thin films established over the past several years for GaAs(100), similar studies were carried out for the GaAs(111)B surfaces. Mapping the GaAs(111)B surface reconstructions and surface "phase diagram" using the RHEED specular beam intensity from static (i.e. non-growing) surfaces, the dynamics of the specular beam was examined under various growth conditions for growths initiated in different regimes of the static surface behavior. The grown films were examined using Nomarski micrographs, scanning electron microscopy, and transmission electron microscopy. The morphological and structural behavior thus found was correlated with the RHEED behavior. Fig. 1 shows the static surface specular beam intensity as a function of the substrate temperature (T_s) at a given As_4 pressure (P_{As4}). The regimes of the surface reconstructions are also identified. It is found that twin-free epilayers with mirror-like surface morphology are reproducibly realized only for growth initiated in the region indicated by the box on the intensity plateau of the $\sqrt{19}$ x $\sqrt{19}$ reconstruction. Fig.2 shows a comparison of a GaAs film grown in this narrow window of optimized growth condition and another grown outside this window. Note the absence of twins and the mirror-like surface of the film grown in the optimized regime. Details may be found in **publications 1 and 2.**

We note that we have, using TEM, examined the nature of the twin defects in the films grown in the non-optimized growth regime, identified these to be a rather interesting double-twin complex, and provided a possible underlying atomistic

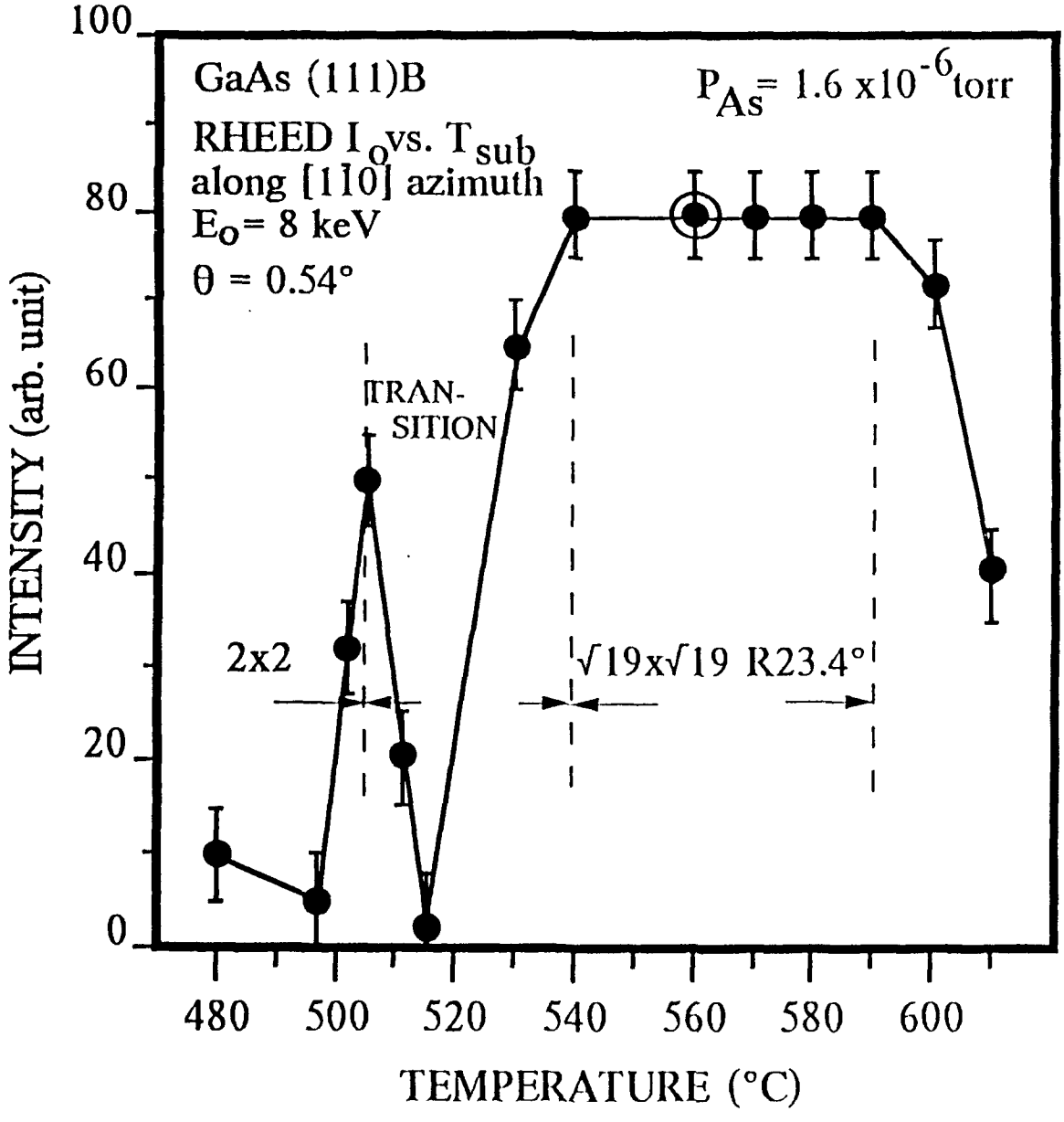
GaAs (111)B
P_{As}= 1.6 x10^{-6}torr
RHEED $I_o$vs. T_{sub}
along [1$\bar{1}$0] azimuth
E_o= 8 keV
θ = 0.54°
TRAN-
SITION
2x2
√19x√19 R23.4°
INTENSITY (arb. unit)
100
80
60
40
20
0
480
500
520
540
560
580
600
TEMPERATURE (°C)

Fig. 1

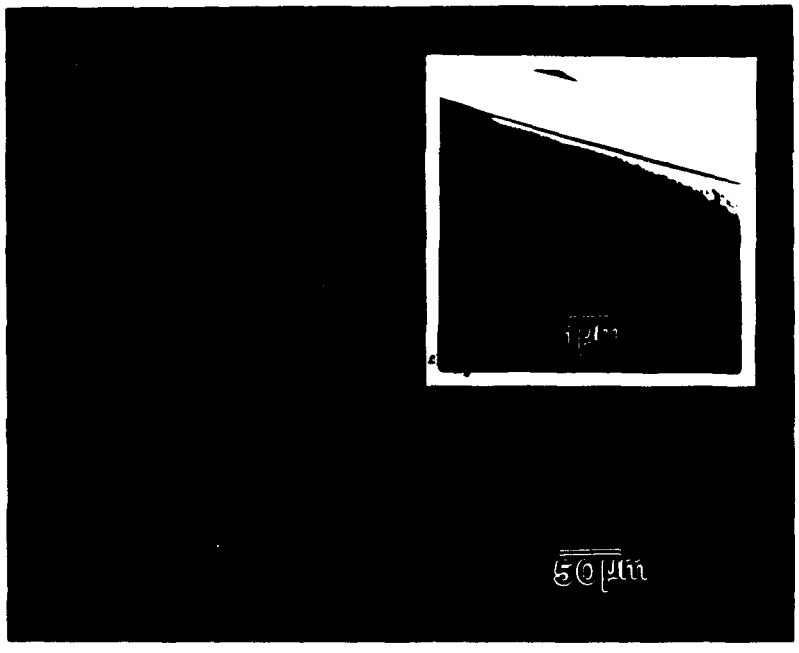

Fig. 2(a) : GaAs (111)B film grown in the RHEED determined optimized region.
Note the mirror-like surface and the absence of twins in the TEM image (inset)

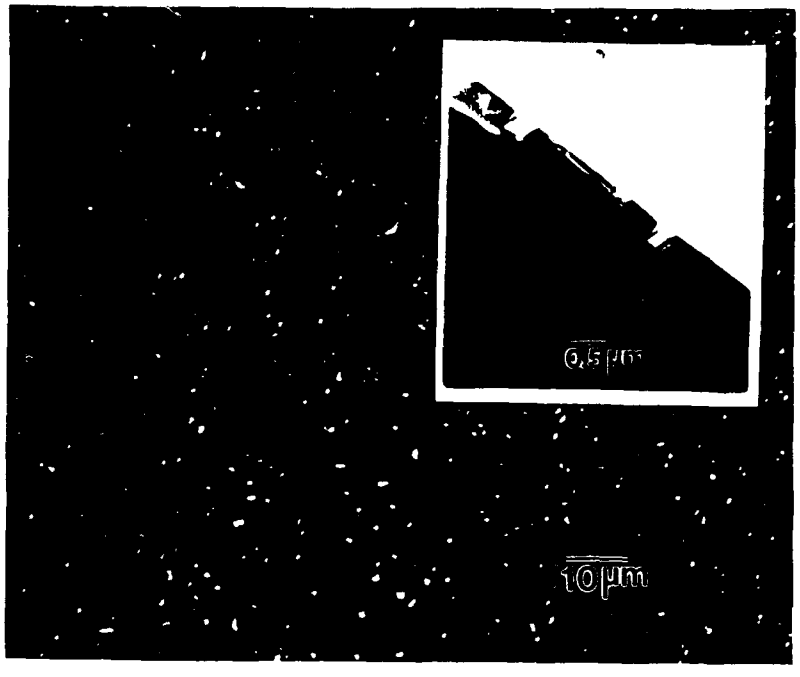

Fig. 2(b) : GaAs (111)B film grown outside the RHEED determined optimized region.

model of Ga and As incorporation during growth which may underlie the occurrence of such defects. Details are provided in **publication 3**. An atomistic model which involves surface kinetics is being examined as a reasonable starting point to examine the atomistic origins of the pyramid-like structures.

I.2 GaAs(100)/$In_xGa_{1-x}As$ HETEROEPITAXY: INITIAL STAGES OF DEFECT FORMATION:

Initial stages of defect formation and strain relaxation in strained heteroepitaxy has been a subject of much interest for some time, the technologically important combinations Si/GaAs, Si/Si_xGe_{1-x} and $GaAs/In_xGa_{1-x}As$ receiving particular attention in recent years. Following our earlier work on the GaAs/InGaAs system, during the present reporting period of the grant we undertook examination of the role of the layer-by-layer and 3D island modes of growth in the onset of incoherency through defect formation at the earliest stages of growth. Since at high lattice mismatch (typically $\geq$ 2%) occurring for In content $\geq$35% the strain induces 3D island formation at the earliest stages ($\leq$ 5ML) of material deposition over much of the deposition condition regime, we paid particular attention to the nature of defects and their formation in the 3D island growth mode regime. Fig. 3 shows a cross-sectional TEM lattice image of 3D islands in a $In_{0.5}Ga_{0.5}As$ film of equivalent thickness of 7 ML deposited at 520°C. Note that small islands (typically < 200A lateral dimensions) are coherent whereas larger islands have lost coherency through the introduction of defects, nearly symmetrically, at the island edges. Although the ambiguities arising from the projection image in cross-sectional TEM prevent

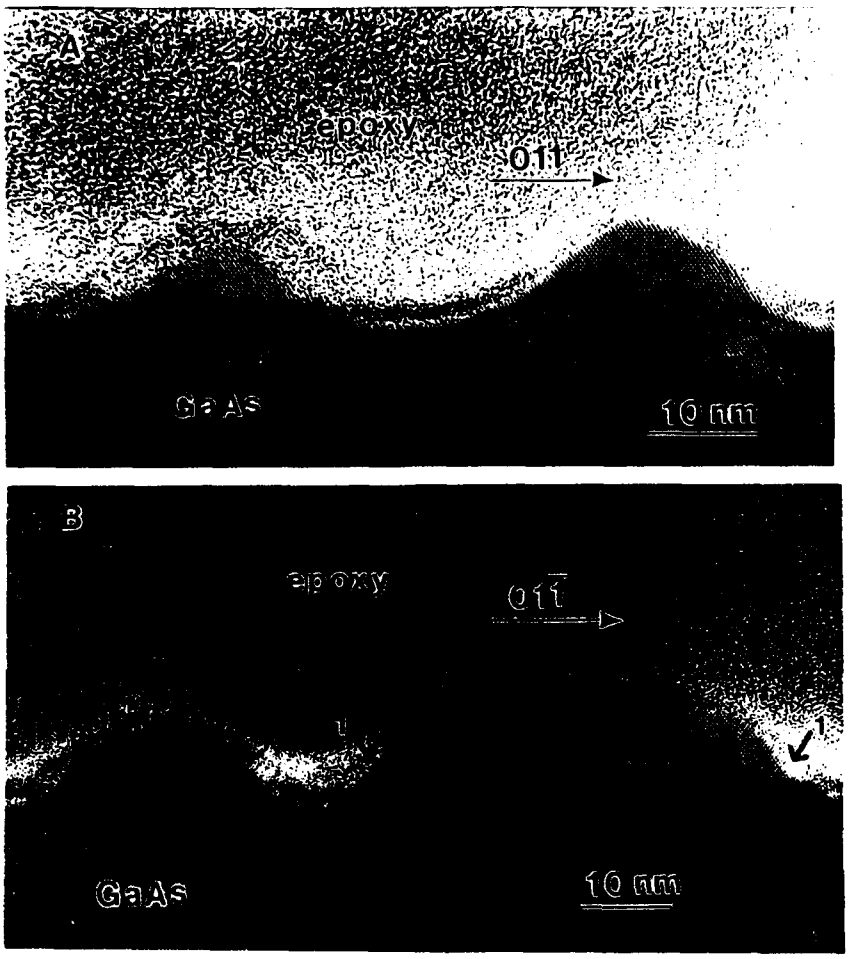

Fig. 3 : Shows coherent and incoherent islands of $In_{0.5}Ga_{0.5}As$ on GaAs (100) in the 3-D island growth mode.

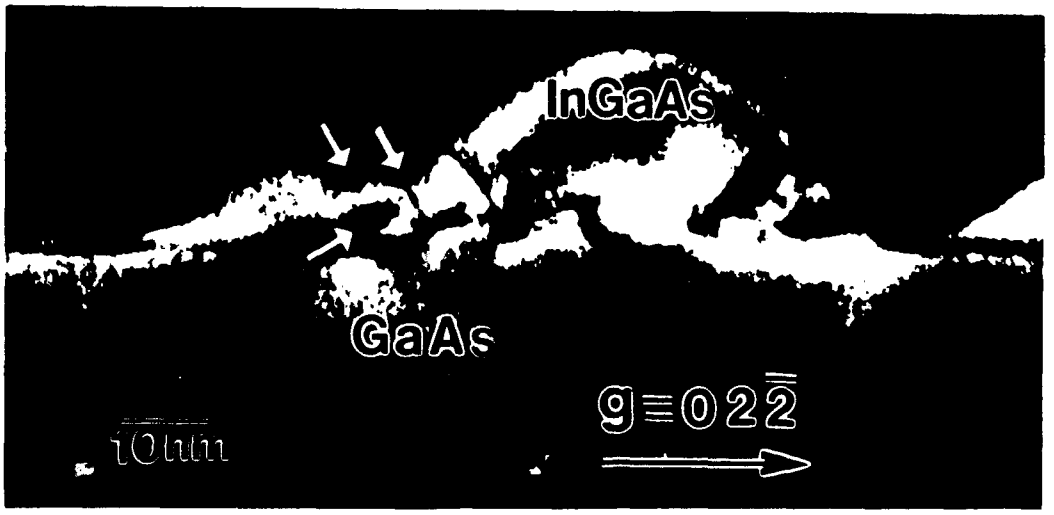

Fig. 4 : A picture suggestive of dislocations forming at cluster coalescence boundaries.

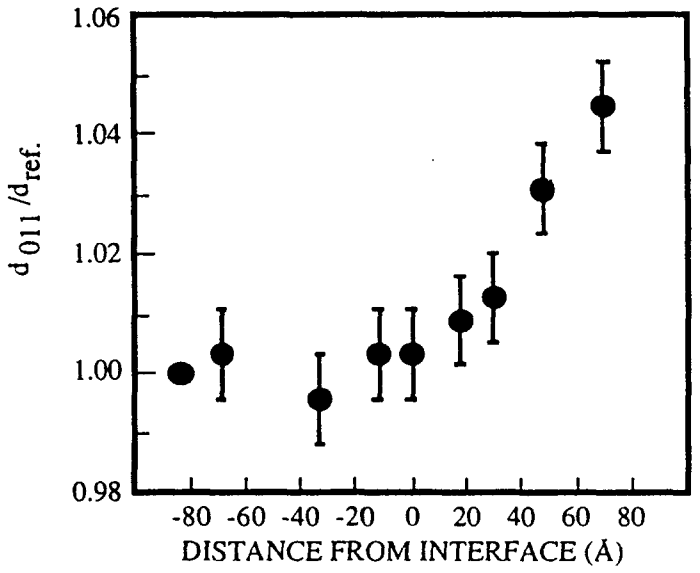

Fig. 5 : Plot of measured $(0\bar{1}1)$ interplanar spacing versus distance from the interface for a coherent island. The interplanar spacing is normalized to the lattice parameter value measured 84 A below the interface in the substrate (d_{ref})

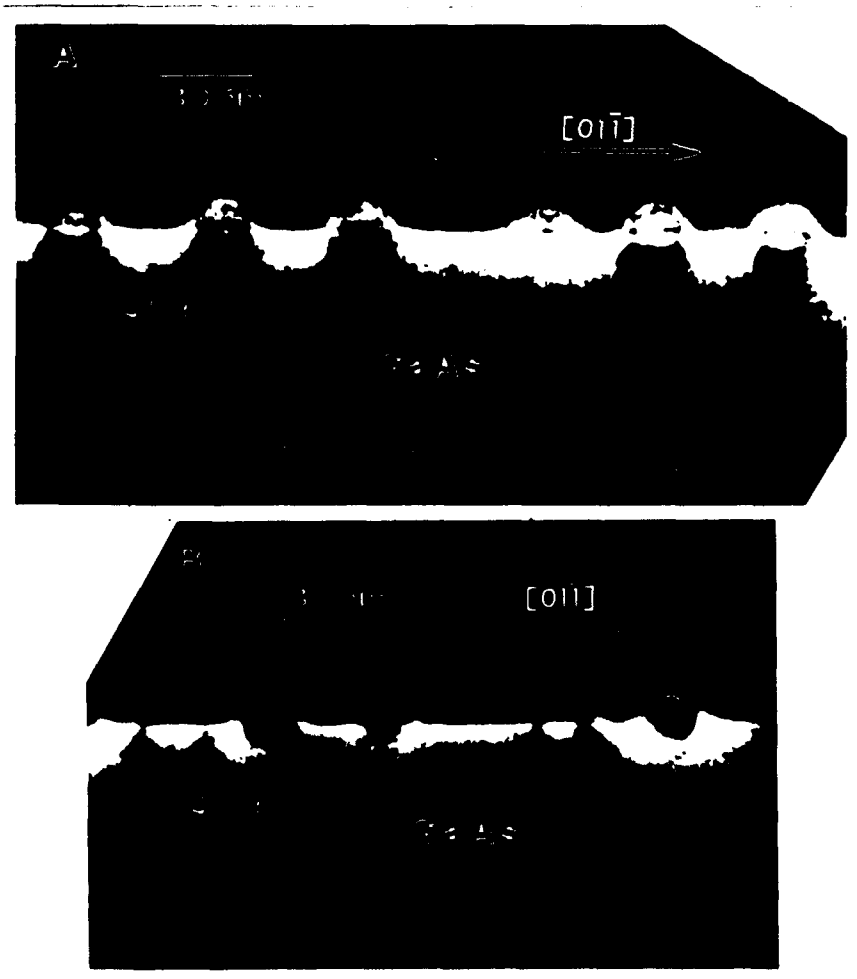

Fig. 6 : Shows existence of strain in the GaAs substrate.

unambiguous conclusion, in a number of cases the location of the defect in relation to the overall island shape is highly suggestive of the possibility that defects are also introduced at the coalescence boundaries of islands. Fig. 4 shows a TEM micrograph of islands suggestive of this mechanism.

Two rather important and **new features** uncovered in these studies are, (i) the existence of **strain relaxation in the islands**, and (ii) the presence of **strain in the substrate** below the islands to large depths of order 150A. Fig. 5 summarizes a typical situation for the former and Fig. 6 shows a TEM micrograph revealing, through strain contrast, the presence of strain in the GaAs(100) substrate. These findings call into question long held (though unsubstantiated) views and historical theories relating to strained epitaxy.

Details of these results and their implications are given in **publications 4, 5 and 6**.

I.3. GaAs(100)/$In_xGa_{1-x}As$/$Al_yGa_{1-y}As$ (y=0 or 1) STRUCTURES:

In this subsection we briefly summarize the findings of **three different types** of GaAs(100)/$In_xGa_{1-x}As$ MBE growths and studies carried out with the objectives of, (i) examining approaches to strain relaxation without the necessity of strain relieving defects, and (ii) realizing high quality electronic and optoelectronic devices in strained GaAs/(InGaAs/AlGaAs) structures grown directly on GaAs(100) substrates without the use of any strain relieving buffers.

I.3.A. PATTERNED GROWTH AND STRAIN RELIEF:

: SINGLE $In_xGa_{1-x}As$ LAYERS

We have previously, under AFOSR sponsored work (AFOSR Grant No. 86-0166), demonstrated the notion that growth of strained layers on substrates containing pre-patterned mesas permits growths to thicknesses as much as seven times those at which dislocations and other extended defects get introduced for growth on non-patterned substrates. The underlying reasoning invoked to expect this was that strain relief was expected to be provided by the presence, at the mesa edges, of the free surface of the grown film. To examine this underlying idea further we undertook growths, on GaAs(100) substrates patterned with mesa stripes down to 1 μm widths, of single epilayers of $In_xGa_{1-x}As$ films with various x and of thicknesses ranging from below to above the nominal critical thickness for dislocation generation on non-patterned substrates. These films were examined via cross sectional TEM and, in collaboration with Drs. Wade Tang and Hal Rosen of IBM Almaden Research Center (San Jose, CA), via micro-Raman scattering measurements to obtain the **spatial variation in the strain across the mesa width**, the side wall growth, and the growths in the valleys between the mesas. Through measurements of the LO and TO phonon induced Raman shifts, relative intensities, the line shapes, and the Stokes-AntiStokes relative intensities, a measure of the spatial distribution of strain and its relation with the TEM observations of the nature of the defects and their density was obtained for the first time. This has provided evidence for the essential correctness of our ideas regarding strain relief in patterned growth. Fig. 7 shows a typical finding for the LO phonon induced Raman shift as

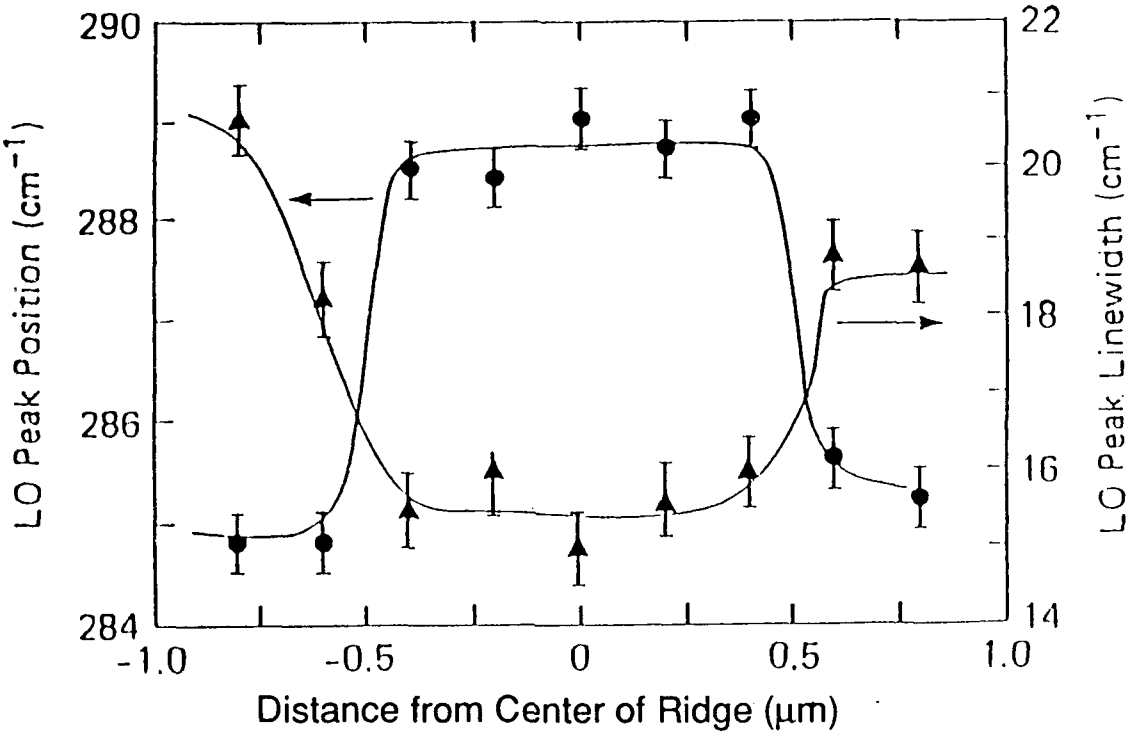
290
288
286
284
22
20
18
16
14
-1.0
-0.5
0
0.5
1.0
LO Peak Position (cm^{-1})
LO Peak Linewidth (cm^{-1})
Distance from Center of Ridge (μm)

Fig. 7

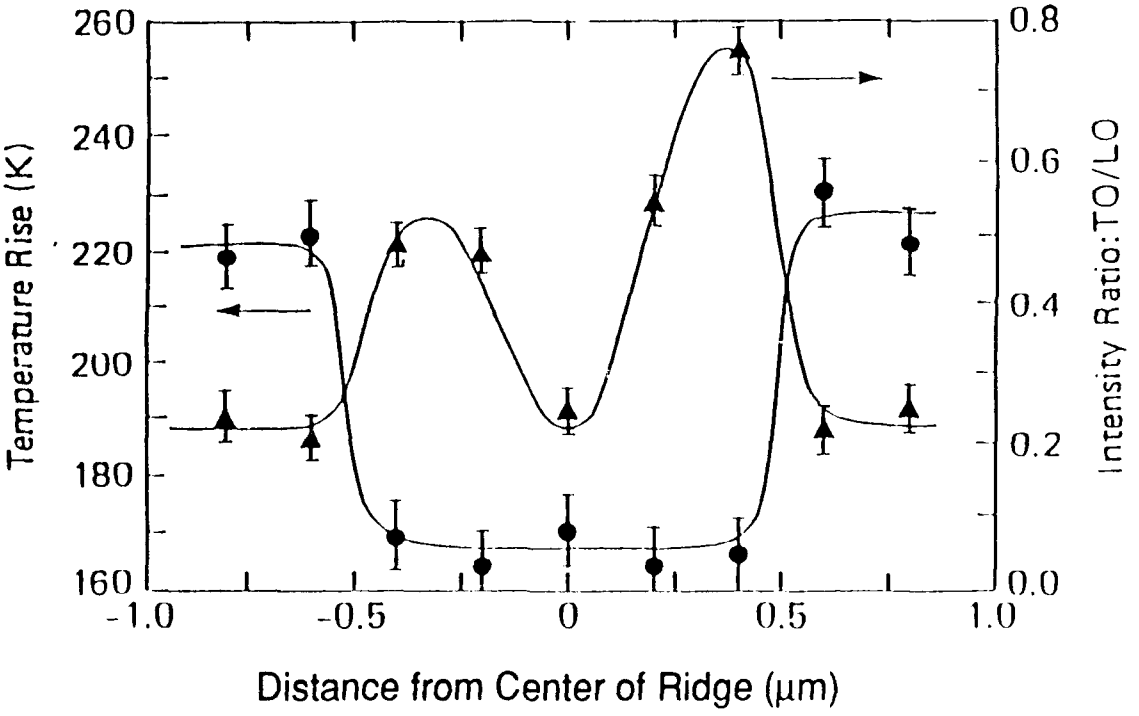
260
240
220
200
180
160
0.8
0.6
0.4
0.2
0.0
-1.0
-0.5
0
0.5
1.0
Temperature Rise (K)
Intensity Ratio:TO/LO
Distance from Center of Ridge (μm)

Fig. 8

one scans across the mesa top into the valley region. Fig. 8 shows the behavior of the temperature rise. Details of these early findings may be found in **publication 7**.

: $GaAs/In_xGa_{1-x}As$ MULTIPLE QUANTUM WELLS:

In addition to the defect reduction and strain variation in single layers of $In_xGa_{1-x}As$ grown on pre-patterned substrates described above, we examined the growth of $GaAs/In_xGa_{1-x}As$ multiple quantum well (MQW) structures on pre-patterned substrates. Since the underlying application oriented motivation in this case derives from use as optical modulators, two aspects on such growths are quite different from the single $In_xGa_{1-x}As$ layer structures discussed above; (1) the total thickness of the MQWs examined has ranged from 1 μm to 2.5 μm, the thickness regime required to obtain sufficient optical interaction path length for applications in light modulation devices based upon the quantum confined Stark effect and the Wannier-Stark localization effect, and (2) the pre-patterned mesas are now rectangular or circular (as opposed to stripes) with linear dimensions varying from 10 μm to 280 μm. The currently envisioned pixel size in a 2-D array of modulator pixels constituting a spatial light modulator (SLM) ranges from 10 μm to 30 μm.

An illustrative example of the possible advantages in the optical properties resulting from growth of highly strained thick MQWs on pre-patterned mesas is represented by the behavior of sample RG 891110. It contains of 100 periods of 80 A $In_{0.2}Ga_{0.8}As$ well and 160 A GaAs barrier layers for a total thickness of ~2.4 μm grown on a substrate containing 16 μm x 18 μm rectangular mesas on 40 μm pitch and, for reference, a nonpatterned region as well. Fig. 9(a) shows a cross sectional

Fig. 9(a) : Shows cross sectional TEM image of the MQW in the nonpatterned region of the GaAs (100) substrate.

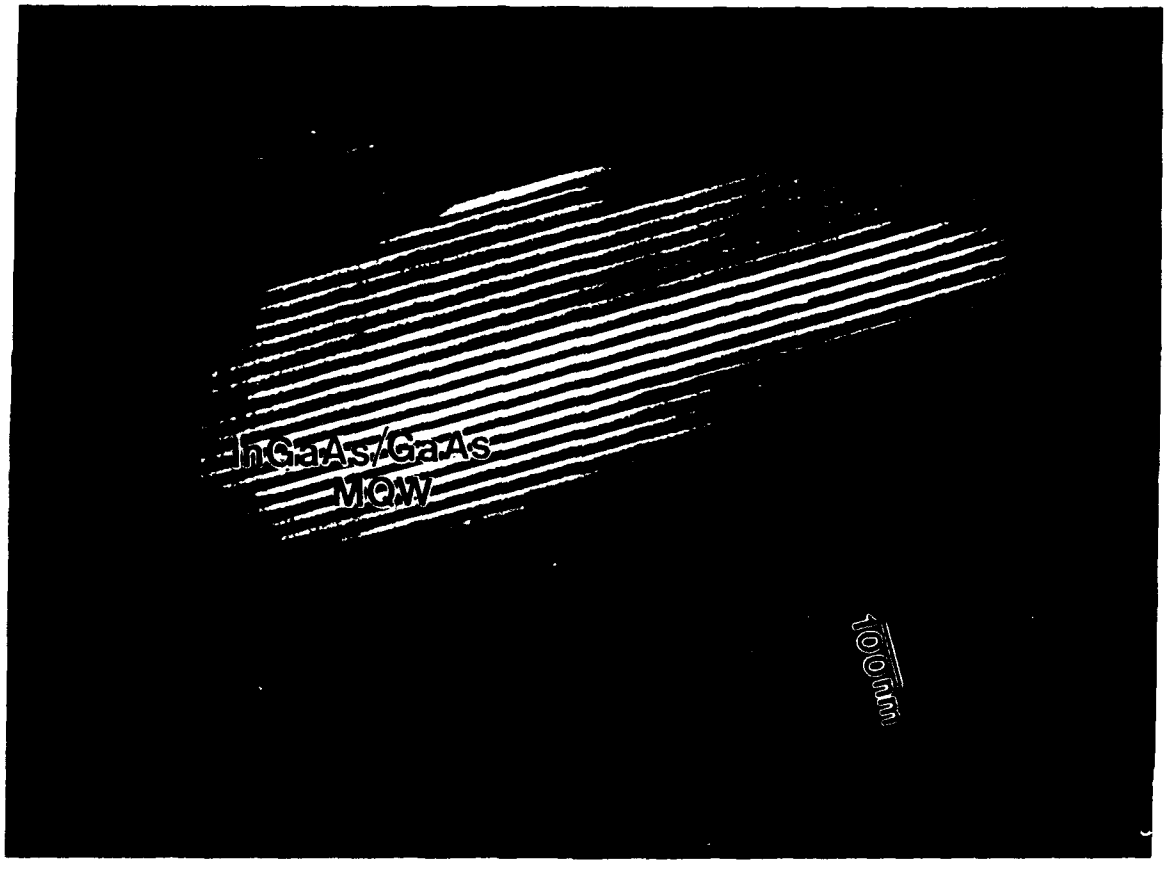

Fig. 9(b) : Shows cross sectional TEM image of the MQW in the central region on top of the prepatterned mesas.

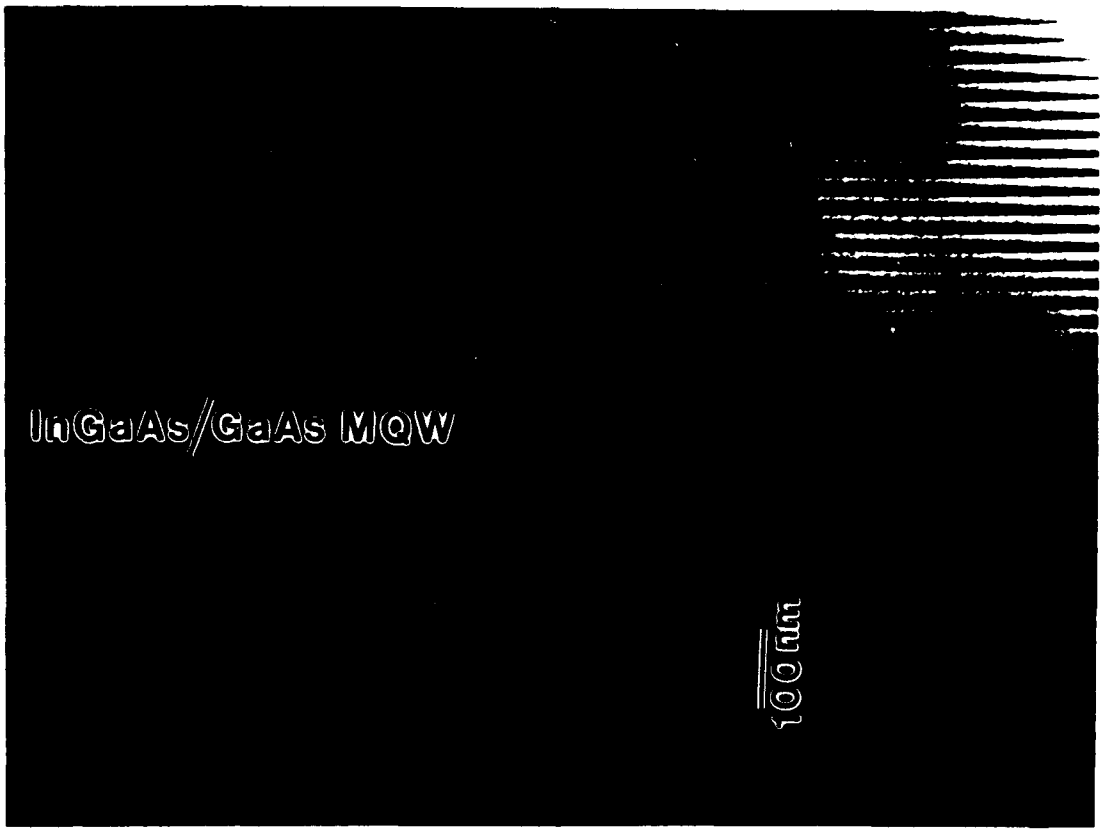

Fig. 9(c) : Shows cross sectional TEM image of the MQW in the central region of the valley between the prepatterned mesas.

TEM image contrast of the nonpatterned regime and, as expected, a high density of threading dislocations and other structural defects is found. By contrast, the central region of the growth on mesa, shown in fig. 9(b), exhibits very high quality of layering with very low defect density. Fig. 9(c) shows the TEM image contrast taken from the region between the mesas. At the level of TEM resolution this region (referred to as the valley region) shows no discernible difference as compared to the meas top. This in itself is surprising for one would have expected a higher defect density, thought perhaps not as high as the nonpatterned region. In fig. 10 is shown the optical absorption behavior of the three regions. While no excitonic features are observed in the nonpatterned region (panel a), consistent with the high density of non-radiative recombination centers implied by the high dislocation density of fig. 9(a), the mesa top (panel b) and valley (panel c) regions show good excitonic features. What is a surprising feature is that the valley region exciton absorption (fig. 10c) is significantly sharper than for the mesa top region and the 6 meV linewidth is comparable to the best photoluminescence linewidth at 20% In composition found in single quantum wells. We are presently examining this unexpected result which could turn out to be of considerable importance in revealing some of the mysteries of strained growth as well as be of practical value in designing SLMs. Given that this work constitutes the first demonstration of the improvement in a physical property of strained MQWs by exploiting the notion of growth on pre-patterned substrates, the initial results were reported in **publication 8**.

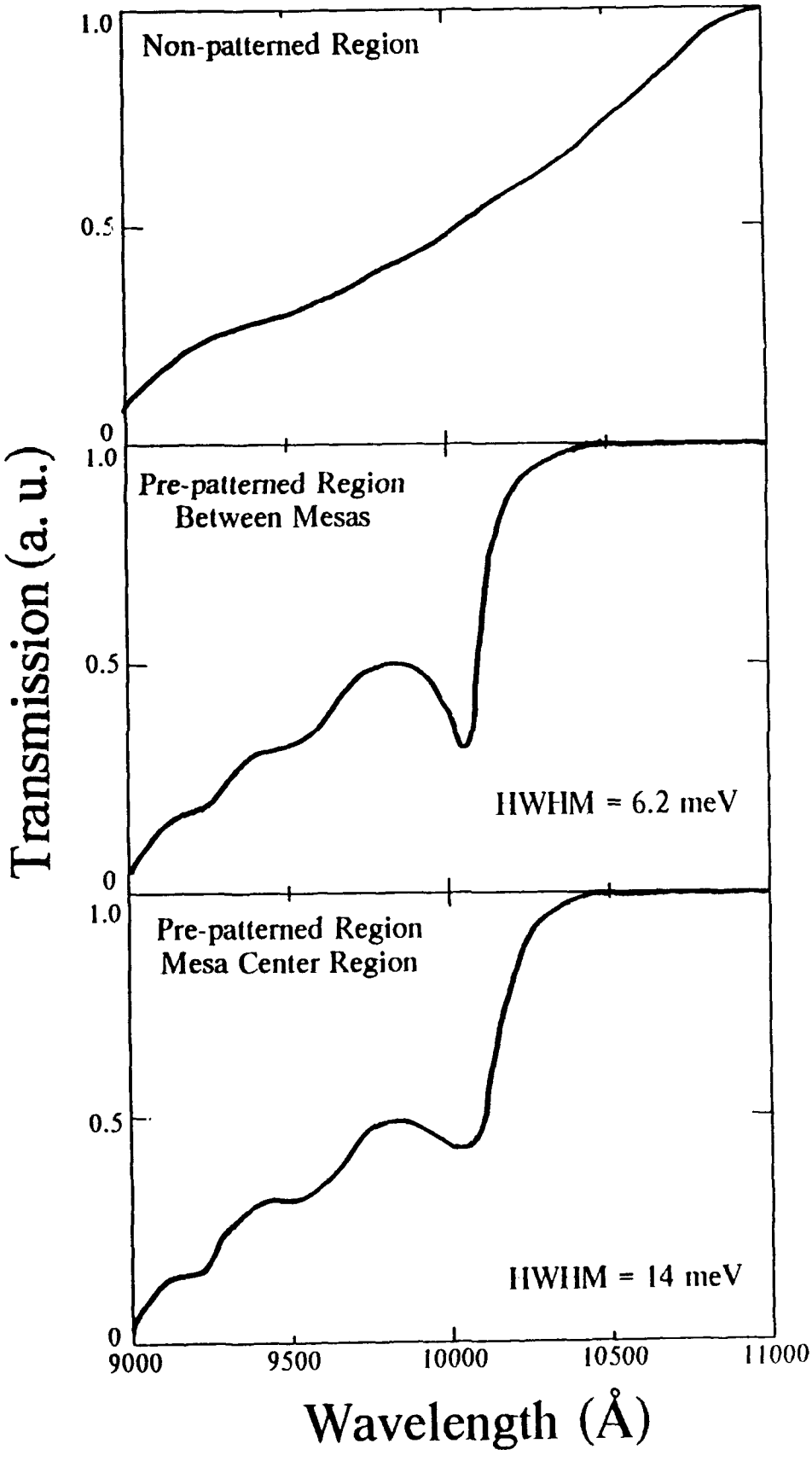
Non-patterned Region
Pre-patterned Region
Between Mesas
HWHM = 6.2 meV
Pre-patterned Region
Mesa Center Region
HWHM = 14 meV
1.0
0.5
0
9000
9500
10000
10500
11000
Transmission (a. u.)
Wavelength (Å)

Fig. 10

I.3.B. RESONANT TUNNELLING DIODES:

Following through on our earlier success in realizing strained $In_xGa_{1-x}As/AlAs$, $x \leq 0.20$ resonant tunnelling structures grown directly on GaAs(100), during the present reporting period we pursued growth of RTD's with $x > 0.25$. This regime is particularly challenging from the MBE growth view point since, depending upon the growth conditions, a change from the layer-by-layer (i.e. 2D) growth mode to 3D island growth mode occurs for x between 0.25 to 0.30. Employing $In_{0.33}Ga_{0.67}As$ alloys as the spacer and well regions and AlAs as the barrier regions and using RHEED determined growth conditions, we were able to control the growth (i.e. suppress 3D islanding) sufficiently well to obtain the results shown in fig. 11. Beyond 33% In suppressing the 3D island formation tendency sufficiently to achieve the degree of interface perfection required by a quantum interference effect based device such as an RTD was not successful. Consequently we turned to exploiting short period multiple quantum wells (SPMQW) of InAs/GaAs as constituting the spacer and well regions, the barrier regions still being AlAs.

In fig. 12 are shown the dc I-V characteristics as well as the cross section electron microscope image contrast of a sample containing $(InAs)_1/(GaAs)_4$ and $(InAs)_1/(GaAs)_2$ SPMQW as the spacer and well regions, respectively. The former thus corresponds to an "equivalent" alloy concentration of 20% and the latter to 33%. One notes a significant improvement of the room temperature peak current density (125 KA/Cm^2 compared to 32 KA/Cm^2 in fig. 11) without any significant loss in the peak-to-valley ratio. Details of these results may be found in **publication 9**.

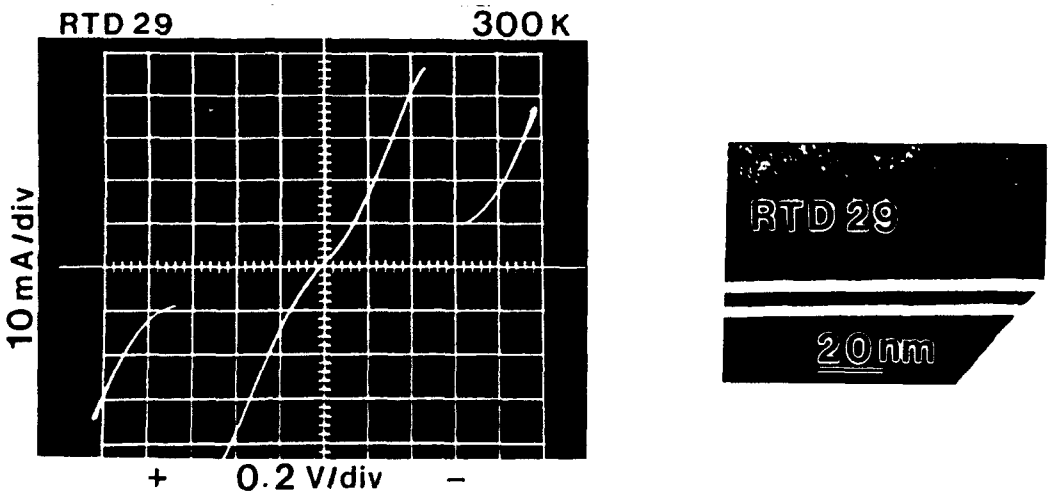

Figure 1. (a) DC I-V characteristics from 12 μm x 12 μm size mesas of RTD #29 with AlAs barriers and conventional alloy $In_{0.3}Ga_{0.7}As$ spacers and well regions. This device shows a J_p of 32 kA/cm^2 with a PVR of 5.2 at 300 K. (b) TEM micrograph of RTD #29 showing highly abrupt and smooth interfaces.

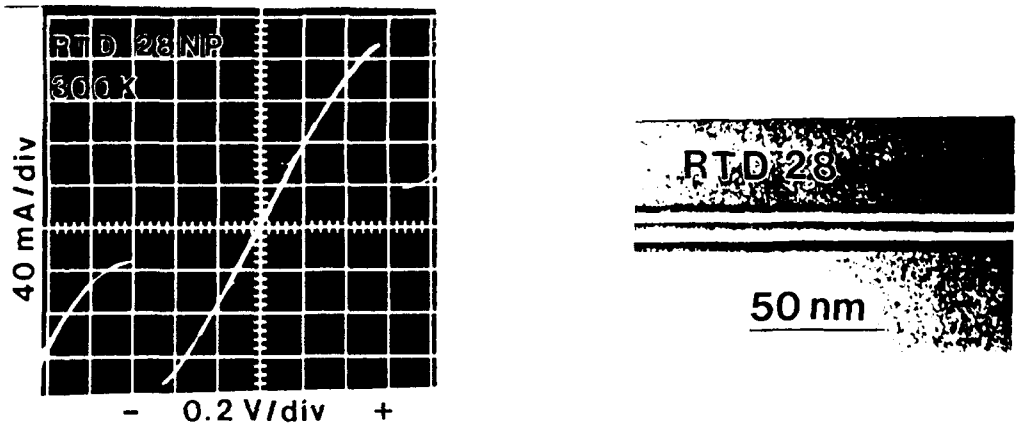

(a) (b)

Figure12 (a) DC I-V characteristics from 12 μm x 12 μm size mesas of RTD #28 with AlAs barriers, short period multiple quantum well (SPMQW) type $In_{0.33}Ga_{0.67}As$ well and SPMQW type $In_{0.2}Ga_{0.8}As$ spacers regions. This device shows a J_p of 125 kA/cm^2 with a PVR of 4.7 at 300 K. (b) TEM micrograph of RTD #28 showing highly abrupt and smooth interfaces.

It may be worth noting that the simultaneously high room temperature peak current density (>100KA/Cm^2) and peak-to-valley ratios ($\geq$5) are not only the best achieved to-date in the strained InGaAs/AlAs system grown directly on the GaAs substrate but are in a regime of practical value. This, combined with the transparent nature of the GaAs substrate for the operating wavelength regime of InGaAs/InAlGaAs based optical devices opens the way for monolithic integration of such RTD's with modulator and detector devices, such as proposed for the monolithic opto-electronic transistor.

I.3.C ELECTRO-ABSORPTION IN MQWs:

The Quantum confined Stark-effect based electroabsorptive and electrorefractive behavior of MQWs offers much potential for realizing appropriate light modulators for digital and analog applications. The strained GaAs/InGaAs based MQW's offer an operating wavelength regime for which the GaAs substrate is transparent, thereby eliminating the necessity of patterned etching of the substrate faced in the GaAs/AlGaAs system when working in the transmission geometry. In the reflection geometry, the transparency of the substrated allows for through-substrate reflection modulators which opens the possibility of a face-to-face bonding between the III-V MQW modulator bearing chip and Si-based detection and addressing circuitry on a Si chip. Motivated by such considerations, during the current reporting period we examined the RHEED based growth conditions for the realization of high quality GaAs/$In_xGa_{1-x}As$ ($x \leq 0.20$) MQW's of total thickness between 1 μm and 1.5 μm grown on n^+ - GaAs(100) non-patterned substrates and

capped with a p^+ GaAs capping layer. The p-i(MQW)-n configuration thus permits application of reverse bias and therefore examination of the absorption behavior under applied electric field as well.

An illustrative example of the room temperature electroabsorption behavior for a 50 period GaAs(70 ML)/$In_{0.13}Ga_{0.67}As$(35 ML) MQW (total thickness 1.486 μm) is shown in fig. 13. Apart from the high quality of the MQW manifest in a remarkably narrow exciton linewidth for such a thick MQW, a feature observed for the first time is the **initial narrowing** of the exciton line up to -4V bias, before broadening sets in due to the well-known tunnelling effect. This revealed, for the first time, that at zero bias the built-in field is highly inhomogeneously distributed through the "intrinsic" MQW region in the p-i(MQW)-n structure - a feature long suspected but never before seen in optical behavior. We thus demonstrated that the zero-bias linewidth in MQW's is not necessarily a true reflection of the intrinsic quality of the sharpness of individual wells but rather manifests the convolution of slightly shifting excitonic transition energy from well to well due to the spatially varying built-in field arising from the background doping. This was confirmed via independent C-V measurements on similar samples which showed that a reverse bias between 4V and 5V was needed to deplete the intrinsic region. The 5.5 meV room temperature linewidth at -4V in fig. 13 narrows to a remarkable 2.5 meV at 77K testifying to the degree of growth control afforded by a systematic and judicious use of RHEED in obtaining kinetically optimized growth conditions.

The inset in fig. 13 shows the maximum change in the absorption coefficient ($\Delta\alpha$) near the zero bias exciton peak and in the tail region as a function of the

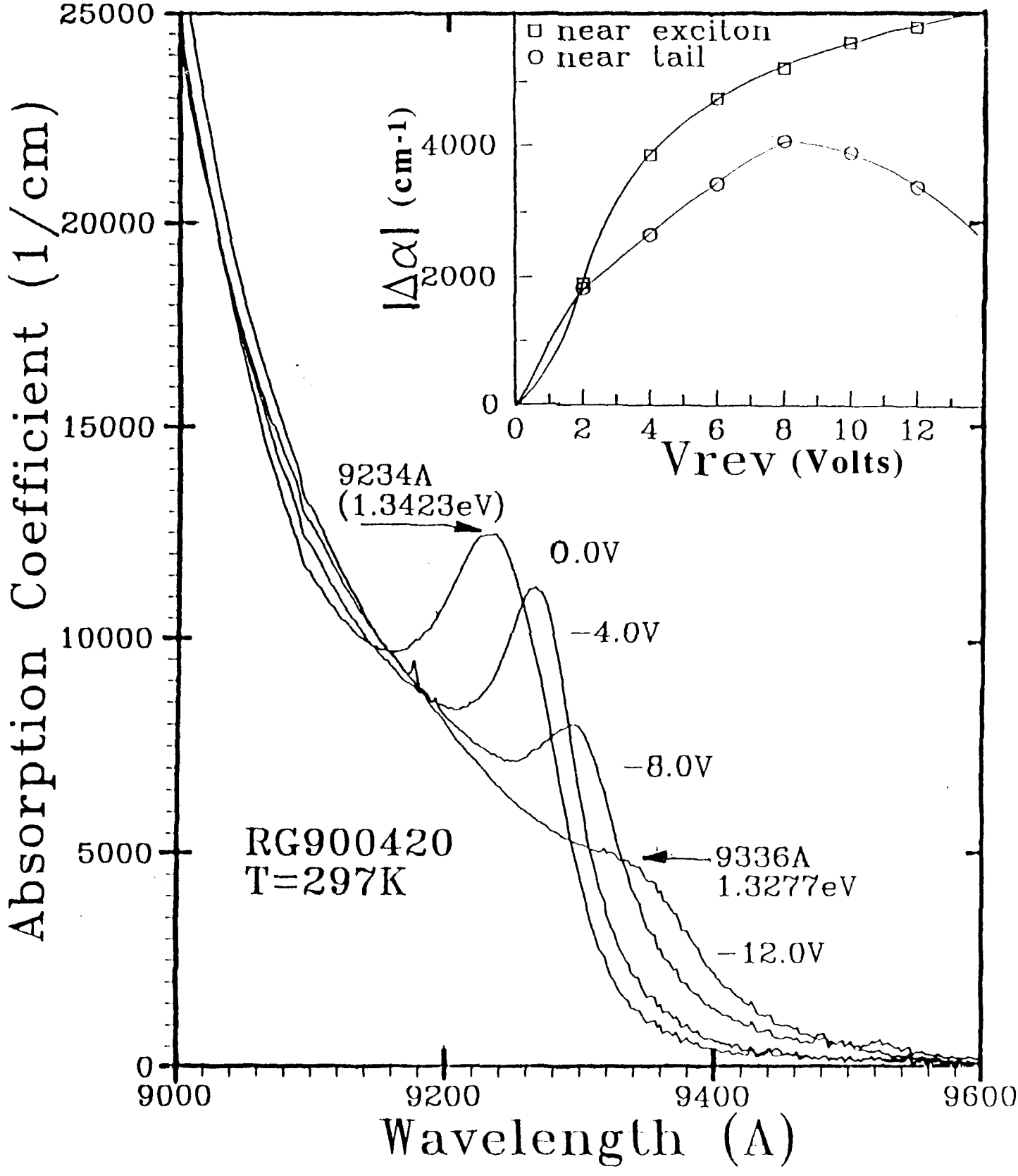
Absorption Coefficient (1/cm)
25000
20000
15000
10000
5000
0
9000
9200
9400
9600
Wavelength (Å)
9234Å
(1.3423eV)
0.0V
−4.0V
−8.0V
9336Å
1.3277eV
−12.0V
RG900420
T=297K
□ near exciton
○ near tail
|Δα| (cm-1)
4000
2000
0
0 2 4 6 8 10 12
Vrev (Volts)

Fig. 13

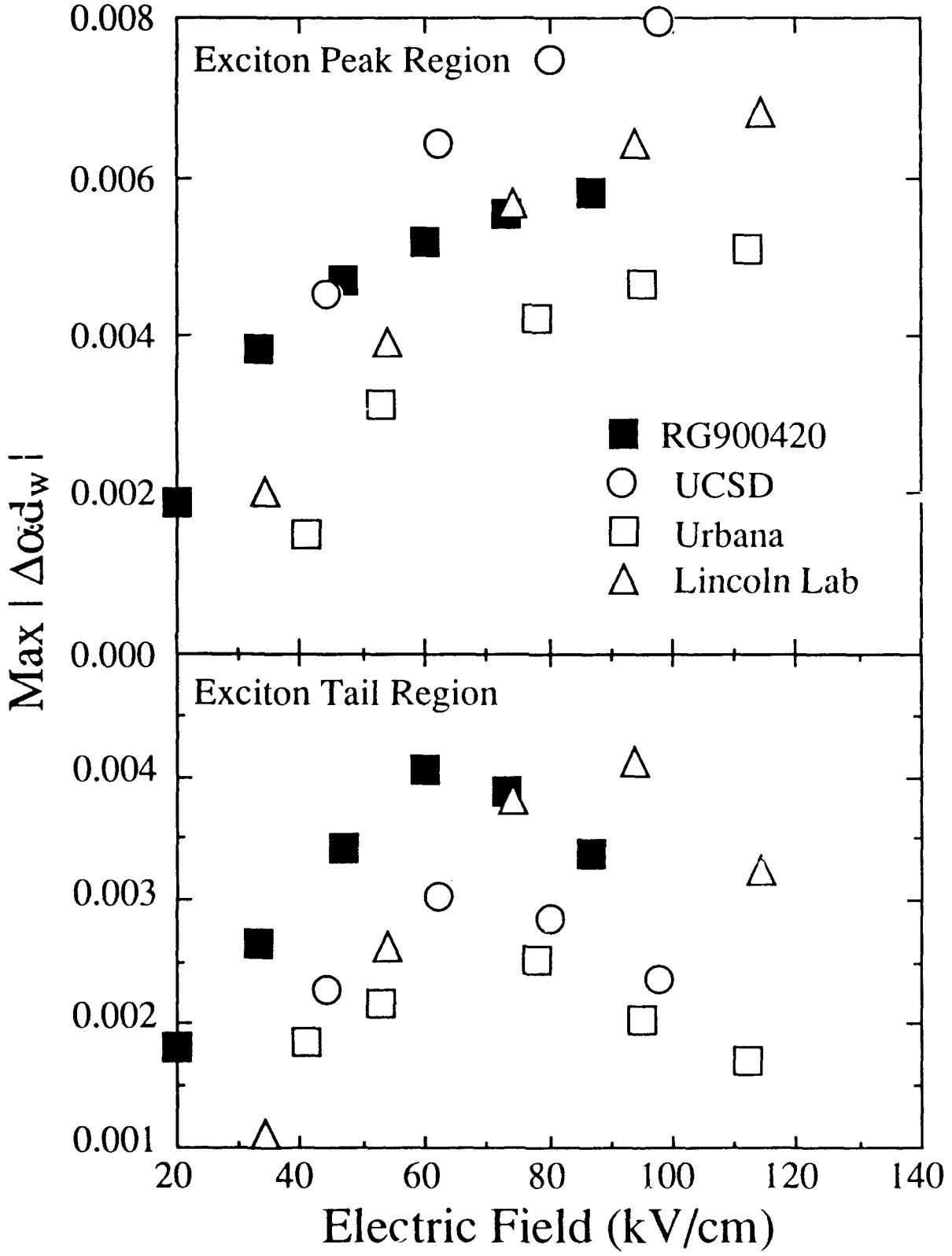
Exciton Peak Region
Exciton Tail Region
RG900420
UCSD
Urbana
Lincoln Lab
Max | Δαd_w |
Electric Field (kV/cm)
0.008
0.006
0.004
0.002
0.000
0.004
0.003
0.002
0.001
20
40
60
80
100
120
140

Fig. 14

applied reverse bias. Finally, in fig. 14 we have summarized the behavior of $\Delta\alpha$ as a function of applied electric field (to achieve normalization with respect to the MQW thickness and accounting for the built-in electric field) for our sample and the other results. As can be seen, at low electric fields - the desired goal for low-drive voltage modulators - the absorption modulation in the exciton tail region - the region of choice for operation of the modulator - is the largest in our sample. Details of these studies may be found in **publications 10, 11, and 12.**

I.4 GaAs(100) / ($In_xGa_{1-x}As$ / $Al_yGa_{1-y}As$) QUANTUM WELLS:

During this reporting period work was initiated on the growth of InGaAs/AlGaAs single and multiple quantum well structures with varying degree of In and Al content. The In content was varied from 0.1 to 0.35 and the Al content from 0 to 1. Besides the usage of InGaAs and AlGaAs alloys as the well and barrier layers, respectively, use of $(InAs)_M$ / $(GaAs)_N$ and $(AlAs)_P$ / $(GaAs)_Q$ short period multiple quantum wells (SPMQW) was also examined. A very important aspect on which work was initiated is the influence of a dielectric encapsulation layer, such as Si_3N_4, on the properties of the underlying strained quantum well structures. This is of particular significance since completion of the as-grown device structure invariably involves such a processing step. In certain cases, rapid thermal annealing (RTA) is also employed as a processing step. In the following we briefly summarize our findings on these aspects during this reporting period.

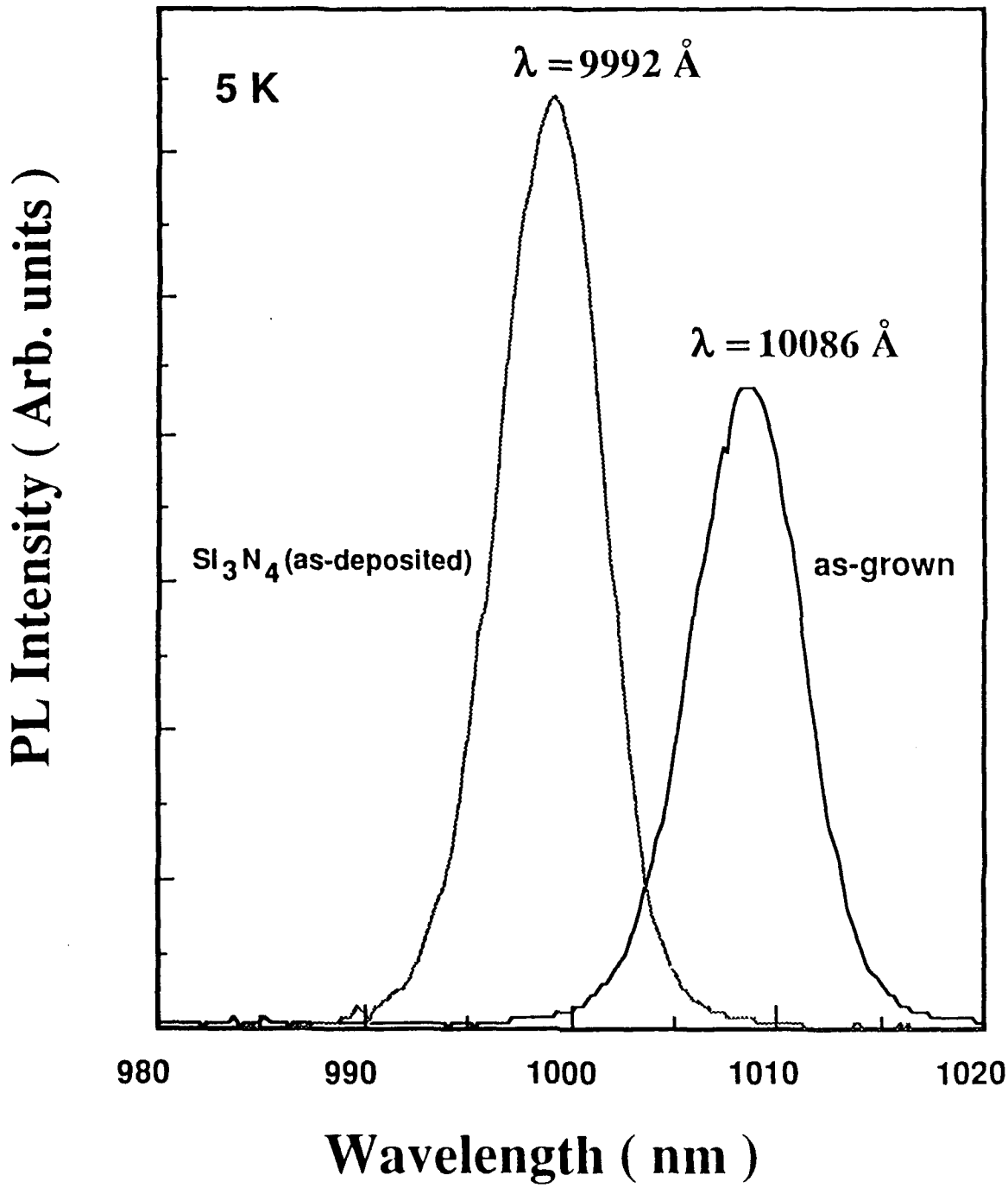
5 K
λ = 9992 Å
λ = 10086 Å
Si3N4 (as-deposited)
as-grown
PL Intensity (Arb. units)
980
990
1000
1010
1020
Wavelength (nm)

Fig. 15

I.4.A. INFLUENCE OF DIELECTRIC ENCAPSULATION:

The as-grown single quantum well structures bearing alloy well and binary compound or alloy barrier layers have given low temperature (5K) PL linewidths as narrow as 5.1 meV for a 145A wide $In_{0.26}Ga_{0.74}As$ well sandwiched between $Al_{0.7}Ga_{0.3}As$ alloy barriers. These are amongst the narrowest linewidths achieved for simultaneously high In and Al bearing structures. Deposition of a Si_3N_4 encapsulation layer (via plasma enhanced chemical vapor deposition) was found to induce a blue-shift in the as-grown exciton position. An Illustrative example is shown in fig.15. The as-grown structure is an asymmetric SQW comprised of a 145A thick $In_{0.26}Ga_{0.74}As$ well sandwiched between GaAs (lower) and AlAs (upper) barriers on which 2000A of PECVD Si_3N_4 layer was subsequently deposited. An exciton blue shift of 94A is observed. The dielectric induced blue shift was observed to be a general feature although the magnitude of the shift is naturally dependent upon the specific structure and, to some extent, the Si_3N_4 deposition conditions. Currently we are examining the view that the Si_3N_4 induces a further strain in concert with the strain already present in the as-grown structure. From the view point of device design the dielectric induced exciton shifts found in these studies caution one to account for such effects.

I.4.B. RAPID THERMAL ANNEALING EFFECTS:

During this reporting period studies of rapid thermal annealing (RTA) of both, the as-grown and Si_3N_4 encapsulated, SQW structures were initiated. For both types of samples, RTA was found to induce a major blue-shift in the exciton

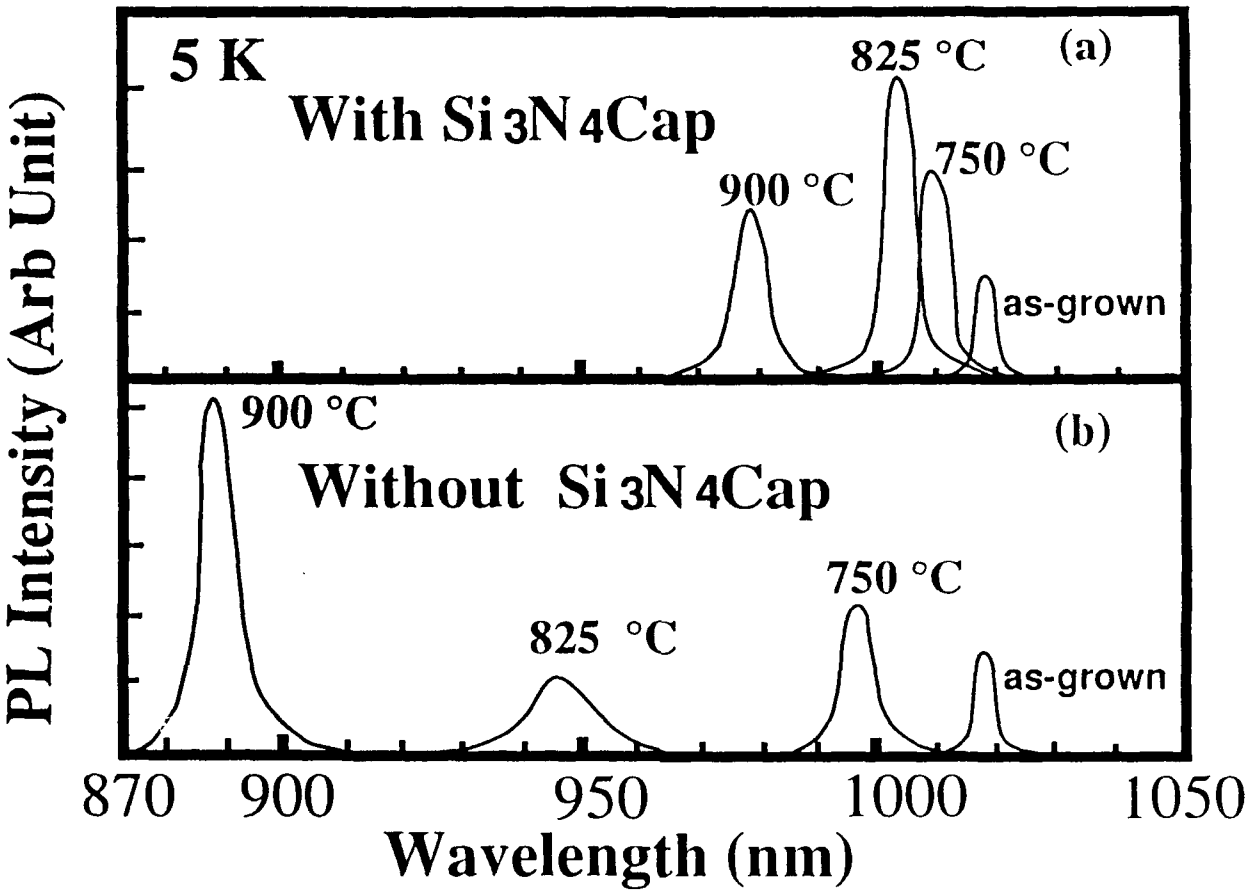
5 K
With Si3N4Cap
825 °C
(a)
750 °C
900 °C
as-grown
900 °C
(b)
Without Si3N4Cap
750 °C
825 °C
as-grown
PL Intensity (Arb Unit)
870
900
950
1000
1050
Wavelength (nm)

Fig. 16

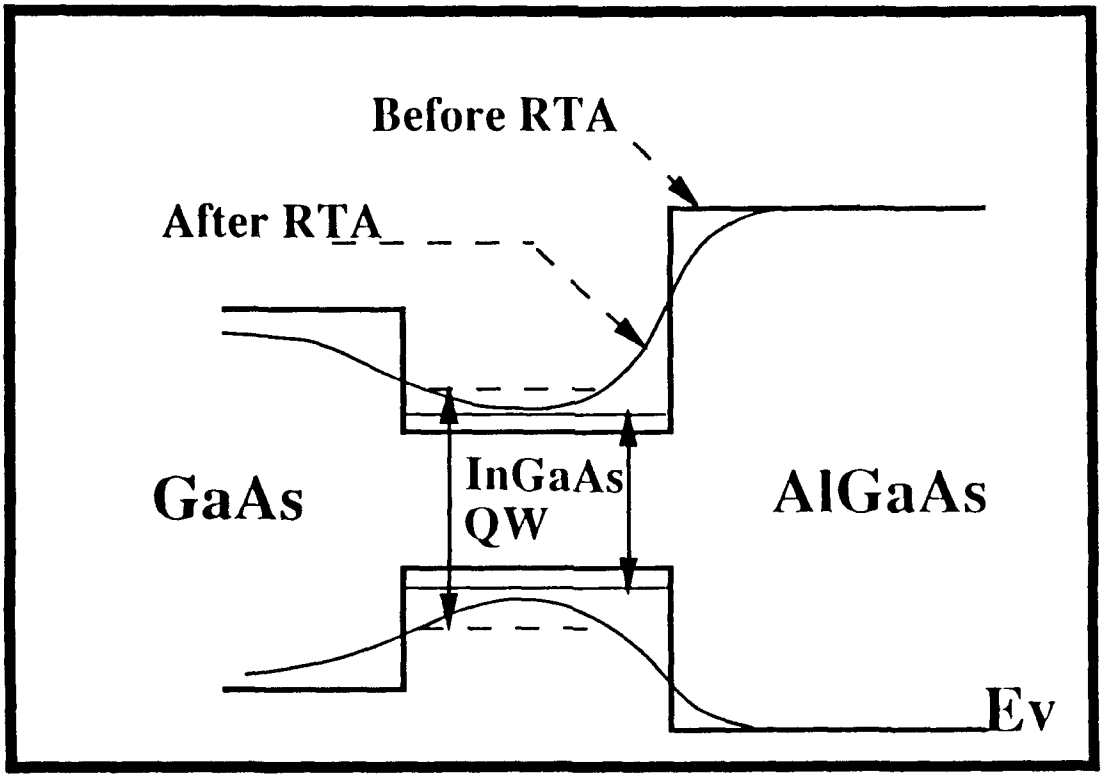
Before RTA
After RTA
GaAs
InGaAs
QW
AlGaAs
Ev

Fig. 17

although the shifts were smaller for the Si_3N_4 encapsulated structures. As an illustration, fig. 16 shows the results for a SQW comprised of a 160A thick $[(In_{0.35}Ga_{0.65}As)_{15}$ / $(GaAs)_4]_3$ as the well layer, GaAs as the lower barrier, and $[(AlAs)_5$ / $(GaAs)_2]_{13}$ short period multiple quantum well as the upper barrier layer. At each RTA temperature shown, both the as-grown and Si_3N_4 encapsulated specimens were exposed to RTA for 6 sec. under ultra high pure N_2 environment. While the exciton blue shifts for the unencapsulated specimen are truly dramatic, they are nevertheless significant for the encapsulated specimen. We take the view that these blue shifts are indicative of cation interdiffusion across the interfaces, particularly the GaAs/InGaAs interface at the lower barrier, induced in the strained metastable structures upon RTA. Such interdiffusion will change the nature of the as-grown quantum well confining potential as illustrated in fig.17, thus giving rise to a blue shift in the exciton position.

II. LIST OF PUBLICATIONS

The following provides a list of publications which have exclusively or substantially benefitted from the support provided under the present contract.

1. K.C. Rajkumar, P. Chen, and A. Madhukar, Jour. Appl. Phys. 69, 2219 (1990).
2. P. Chen, K.C. Rajkumar and A. Madhukar, Appl. Phys. Letts. 58, 1771 (1991).
3. K.C. Rajkumar, P. Chen, and A. Madhukar, in the Proceedings of the 20th ICPS Conference (Aug. 1990, Thessaloniki, Greece), Eds. E.M. Anastassakis, J.D. Joannopoulos, (World Scientific, Singapore), Vol.1, p.276 (1990).
4. S. Guha, A. Madhukar and K.C. Rajkumar, Appl. Phys. Letts. 57, 2110 (1990).
5. S. Guha, K.C. Rajkumar and A. Madhukar, Jour. Cryst. Growth, Vol. 111 (1991).
6. S. Guha, A. Madhukar, R. Kapre and K.C. Rajkumar, Proc. of MRS Fall 1990 Meeting (Boston, Mass), In Press.
7. W.C. Tang, H. Rosen, S. Guha and A. Madhukar, Appl. Phys. Letts. 58, 1644 (1991).
8. A. Madhukar, K.C. Rajkumar, Li Chen, S. Guha, K. Kaviani, and R. Kapre, Appl. Phys. Letts. 57, 2007 (1990).
9. R. Kapre, A. Madhukar and S. Guha, Appl. Phys. Letts. 58, 2255 (1991).
10. Li Chen, K.C. Rajkumar, and A. Madhukar, Appl. Phys. Letts. 57, 2478 (1990).
11. Li Chen, A. Madhukar, K.C. Rajkumar, K.Z. Hu, and J.J. Jung, Proceedings of the 20th ICPS Conference (Aug. 1990, Thessaloniki, Greece), Eds. E.M. Anastassakis, J.D. Joannopoulos, (World Scientific, Singapore) Vol. 2, p. 1117 (1990).
12. Li Chen, K.C. Rajkumar, A. Madhukar, Wei Chen, S. Guha and K. Kaviani, Jour. Cryst. Growth (In Press).

13. P. Chen, K.C. Rajkumar, and A. Madhukar, J. Vac. Sc. Tech. B9, 2312 (1991).

III. CONFERENCE PRESENTATIONS

1. K.C. Rajkumar, P. Chen, and A. Madhukar, 20th ICPS Conference, Aug. 1990, Thessaloniki, Greece.
2. Li Chen, A. Madhukar, K.C. Rajkumar, K.Z. Hu, and J.J. Jung, 20th ICPS Conference, Aug. 1990, Thessaloniki, Greece.
3. S. Guha, K.C. Rajkumar and A. Madhukar, 6th International MBE Conference, Aug. 1990, San Diego, CA.
4. Li Chen, K.C. Rajkumar, A. Madhukar, Wei Chen, S. Guha and K. Kaviani, 6th International MBE Conference, Aug. 1990, San Diego, CA.
5. P. Chen, K.C. Rajkumar, and A. Madhukar, PCSI 20 Conference in Long Beach, CA, Jan. 1991.
6. S. Guha, A. Madhukar, R. Kapre and K.C. Rajkumar, MRS Fall 1990 Meeting, Boston, Mass.

V. PERSONNEL:

GRADUATE STUDENTS (supported fully or partially)

1. Supratik Guha (Ph.D., Jan. 1991)
2. R.M. Kapre (Ph.D. expected May 1991)
3. Li Chen (Ph.D. expected Dec. 1991)
4. K.C. Rajkumar (Ph.D. expected May 1992)

POST-DOCTORAL VISITORS

1. Dr. Ping Chen